IET Communications

Research Article

# Low-complexity peak-to-average power ratio reduction method for orthogonal frequency-division multiplexing communications

ISSN 1751-8628
Received on 7th November 2014
Revised on 21st July 2015
Accepted on 11th August 2015
doi: 10.1049/iet-com.2015.0194
www.ietdl.org

*Yuewen Wang* ✉, *Ali N. Akansu*

*Department of Electrical and Computer Engineering, New Jersey Institute of Technology, Newark, NJ 07102, USA*
✉ *E-mail: yw46@njit.edu*

**Abstract:** The high peak-to-average power ratio (PAPR) of the transmitted signal is a major drawback of multicarrier transmission such as orthogonal frequency-division multiplexing OFDM. A plethora of PAPR reduction techniques has been reported in the literature. Some of the techniques modify the phase and/or amplitude of symbols in the original symbol alphabet (SA) such as selected mapping and partial transmit sequences techniques. However, such methods have shortcomings of a heavy computational burden caused by required multiple inverse fast-Fourier transform (IFFT) operations and bit error rate performance degradation due to side information (SI). In this study, a low-complexity PAPR reduction framework is proposed to jointly modify phase and amplitude values of the original symbols in the alphabet. This framework utilises only one IFFT/FFT operator pair for transmultiplexing of symbols without any SI. The merit of the proposed method to design a SA modifier matrix (SAM) for PAPR reduction is shown through performance comparisons for the application scenarios presented in this study.

## 1 Introduction

Multicarrier transmission such as orthogonal frequency-division multiplexing (OFDM) has been successfully used in various wireless communication technologies. The OFDM system brings the advantages of avoiding frequency selective fading, narrow band interference and inter-symbol interference [1, 2]. The easy implementation of this system, by using fast Fourier transform (FFT), is also quite attractive. However, the OFDM signal is a sum of orthogonal frequency modulated subcarriers. When subcarriers weighted with the corresponding symbol values are added coherently, the resulting high peak-to-average power ratio (PAPR) becomes a major drawback of the OFDM systems due to reduced power efficiency in radio frequency power amplifier (PA) and digital-to-analogue converter (DAC) modules. High PAPR prevents the PA from operating within its linear region, causes additional interference, and induces bit error rate (BER) performance degradation. Moreover, it demands a wider dynamic range in DAC to accommodate the large peaks of the OFDM frame (signal). Such a situation leads to inefficient amplification and increases the cost of the system. Therefore, PAPR reduction techniques play an essential role to improve power efficiency in the OFDM systems.

There has been a variety of PAPR reduction methods emphasising different aspects proposed in the literature [3]. One typical technique of these approaches modifies the original symbol alphabet (SA) through phase rotation and/or amplitude change pre- or post-inverse FFT (IFFT) operator in order to reduce PAPR. The representational techniques such as partial transmit sequences (PTS) [4, 5], selective mapping (SLM) [6, 7] and Walsh–Hadamard transform (WHT) [8] methods have been widely used for such a task. Although the PTS and SLM methods provide PAPR reduction, their computational complexity and implementation cost with utilisation of multiple IFFT operators are relatively high. In addition, for a set of OFDM signal candidates used in the PTS and SLM methods, some bits of side information (SI) must be transmitted error-free to the receiver along with the OFDM frame in the system. There are extensions of SLM [9–12] and PTS [13, 14] that also modify power levels of symbols in the alphabet in order to reduce PAPR [10, 11] or to eliminate SI [14–17]. The WHT method improves PAPR without any power increase and SI requirement in a low-complexity system, but with a less PAPR reduction compared to the SLM and PTS methods.

The trade-off for PAPR reduction in the existing methods is either increased average power and/or added computational complexity. A new PAPR reduction scheme is proposed in this paper that implements a pre-designed SA modifier (SAM) matrix to change the amplitude and phase values of the original data symbols prior to the IFFT operation of an OFDM system at the transmitter. The receiver can recover original data symbols by employing the corresponding inverse SAM after FFT without BER degradation. The proposed method is a marked departure from the existing ones and offers a simple framework devised to be independent of original data symbols, formulates PAPR reduction problem elegantly and outperforms PTS, SLM and WHT precoded OFDM (WHT-OFDM) significantly for the communication scenarios considered in this paper.

The PAPR in OFDM communication systems and popular PAPR reduction methods are briefly reviewed in Section 2. The motivation and design procedure of the proposed method are described in Section 3. The performance comparisons of various methods are presented in Section 4. Then, the concluding remarks of the paper are given Section 5.

## 2 PAPR in OFDM communications

An OFDM frame is generated by the multiplexing of independent symbols modulated with orthogonal frequency subcarriers. The incoming data bit stream is modulated into a sequence of symbols from the predefined SA of $M$-ary phase-shift keying ($M$-PSK) or $M$-ary quadrature amplitude modulation ($M$-QAM) that populate the symbol vector $\underline{\boldsymbol{X}} = [X(0), X(1), \ldots, X(N-1)]^{\mathrm{T}}$, where $[\cdot]^{\mathrm{T}}$ denotes a transpose operator, $N$ is the number of subcarriers employed. $M$ is the power of 2 such as 4 (QPSK), 8 (8-PSK), 16 (16-QAM) and so on. The continuous-time baseband multicarrier signal is the summation of $N$ subcarriers weighted by symbols and expressed as [3]

$$x(t) = \frac{1}{\sqrt{N}} \sum_{k=0}^{N-1} X(k) \mathrm{e}^{\mathrm{j}2\pi f_k t}, \quad 0 \le t < N t_{\mathrm{s}}. \tag{1}$$

Subcarriers are orthogonal where $f_k = k\Delta f$, $\Delta f = 1/Nt_s$, $t_s$ is the symbol period and $j = \sqrt{-1}$. Then, the discrete-time OFDM frame is the sampled version of (1) at the *Nyquist rate* $t = nt_s$ and written as

$$x(n) = \frac{1}{\sqrt{N}} \sum_{k=0}^{N-1} X(k) e^{j2\pi kn/N}, \quad n = 0, 1, \ldots, N-1. \tag{2}$$

Let $\underline{x} = [x(0), x(1), \ldots, x(N-1)]^T$ denotes the resulting discrete-time OFDM frame in a vector form. The PAPR of an OFDM frame due to signal amplitude fluctuation is defined as

$$\text{PAPR} = \frac{\max_{n=0,1,\ldots,N-1} |x(n)|^2}{E\left[|x(n)|^2\right]}, \tag{3}$$

where $E[\cdot]$ denotes the expectation operator.

The complementary cumulative distribution function (CCDF) is a commonly used measure to evaluate PAPR performance [18]. The CCDF of the PAPR indicates the probability that the PAPR of a signal exceeds a given threshold, i.e. $\Pr\{\text{PAPR} > \text{PAPR}_0\}$.

The PTS and SLM techniques are a probabilistic algorithm to reduce the possibility of high PAPR by generating several candidate OFDM frames representing the same symbol vector and selecting the one with the lowest PAPR prior to transmission. In the SLM method, duplicates of original data symbols (symbol vector components) are symbol-wisely multiplied with $U$ different phase-shifting sequences (phase modifiers) $\underline{B}^u = e^{j\theta^u}$, $\theta^u \in [0, 2\pi)$, where phase sequence has the same length of data symbols. After going through IFFT operators individually, the modified OFDM frame with the minimum PAPR among all candidates is identified and transmitted to the receiver [6]. In the PTS method, similar to the SLM, a set of $V$ sub-blocks partitioned from the original data symbol vector are first multiplexed by the IFFTs individually. Then, the lowest PAPR signal is generated by optimally combining these sub-blocks with phase shifting coefficients selected from $W$ complex elements [5]. Therefore, a set of IFFT operators are required for all candidate OFDM frames at the transmitter both in the SLM and PTS methods. Moreover, SI per OFDM frame are demanded to be sent to the receiver in an error-free fashion for the purpose of recovering original data symbols with the corresponding phase-shifting sequence/coefficients by receiving SI correctly. There are extensions of the SLM technique which modify phase and also amplitude in the original SA [9–11]. An extended SLM technique, without SI, jointly utilising modified phase and amplitude with sequence $\underline{P}^u = (De^{j\pi})^{\underline{p}^u}$, $\underline{p}^u \in \{0, 1\}$ and $D$ as a magnitude extension factor, was proposed in [9]. This amplitude modified SLM (A-SLM) technique recognises the selected phase sequence by calculating Hamming distance to estimate the location of magnitude extension factors. However, this method increases the total transmit signal power. In the WHT-OFDM system [8], the original symbol vector is transformed by WHT before passing through the IFFT block at the transmitter without increasing power. However, its PAPR performance is inferior to the SLM and A-SLM methods.

## 3 Symbol alphabet modifier method

We herein introduces a low complexity PAPR reduction method for the OFDM systems that jointly modifies phase and amplitude of the original SA such as $M$-PSK and $M$-QAM.

The difference between peak power and mean power that is expressed as $\left|\max_{n=0,1,\ldots,N-1} |x(n)|^2 - E[|x(n)|^2]\right|$ should be minimised by any PAPR reduction method. In the ideal case, all components of OFDM frame vector $\underline{x}$ having the same amplitude can make the PAPR to be **1** and the power difference to be zero. The design motivation for a proper SAM is first to find such an $N \times N$ matrix $\boldsymbol{C}^{-1}$ instead of the inverse discrete Fourier transform (DFT) matrix $\boldsymbol{A}_{\text{DFT}}^{-1}$ that can map a symbol vector into an OFDM frame with constant amplitude components. Here superscript '−1' is used to indicate the inverse matrix such that all matrices designed at the transmitter are identical to the denotation of the inverse DFT matrix $\boldsymbol{A}_{\text{DFT}}^{-1}$ and implied to be invertible, vice versa at the receiver. Hence, it is necessary to define the design constraints such that the matrix $\boldsymbol{C}^{-1}$ must be invertible at the receiver and factorable to the $\boldsymbol{A}_{\text{DFT}}^{-1}$ matrix which served as the frequency selective orthogonal multiplexer. The design steps are explained as follows:

(a) First, define an $N \times N$ transform matrix $\boldsymbol{C}^{-1}$ as

$$\boldsymbol{C}^{-1} = [c_n(k)] = [\alpha_{k,n} \cdot e^{j\varphi_n(k)}], \quad k, n = 0, 1, \ldots, N-1, \tag{4}$$

where amplitudes of matrix elements $\alpha_{k,n} \in \mathbb{R}^+$, $k$ and $n$ denote for column and row indices of a matrix. Then, the OFDM frame is expressed as

$$x(n) = \sum_{k=0}^{N-1} c_n(k) X(k), \quad n = 0, 1, \ldots, N-1, \tag{5}$$

and the amplitude of each component is calculated as

$$|x(n)| = \left| \sum_{k=0}^{N-1} c_n(k) X(k) \right|. \tag{6}$$

Then, by inspection, we force the equality of arbitrary two components in an OFDM frame as the following relationship

$$\begin{gathered} |x(m)| = \left|e^{j\Delta\phi_{m,n}} \cdot x(m)\right| = |x(n)| \\ x(n) = \sum_{k=0}^{N-1} c_m(k) e^{j\Delta\phi_{m,n}} \cdot X(k) \\ m, n = 0, 1, \ldots, N-1, m \neq n, \end{gathered} \tag{7}$$

where $\Delta\phi_{m,n}$ denotes the phase difference between the $n$th and the $m$th components of OFDM frame vector. From (7), an intuitive design of the $n$th and the $m$th rows of matrix $\boldsymbol{C}^{-1}$ is as follows

$$\begin{aligned} c_n(k) &= c_m(k) \cdot e^{j\Delta\phi_{m,n}}, \quad n \neq m, \ k = 0, 1, \ldots, N-1 \\ &\Rightarrow \alpha_{k,n} \cdot e^{j\varphi_n(k)} = \alpha_{k,m} \cdot e^{j\varphi_m(k)} \cdot e^{j\Delta\phi_{m,n}} \\ &\Rightarrow \alpha_{k,n} = \alpha_{k,m} = \alpha_k, \\ &\quad \varphi_n(k) = \varphi_m(k) + \Delta\phi_{m,n} = \varphi(k) + \Delta\phi_n, \end{aligned} \tag{8}$$

where $\Delta\phi_n = \Delta\phi_{0,n}$, $\varphi(k) = \varphi_0(k)$ is the phase of the $k$th element in the first row ($m = 0$) of the matrix $\boldsymbol{C}^{-1}$.

(b) Now, we can express $\boldsymbol{C}^{-1}$ as

$$\boldsymbol{C}^{-1} = [c_n(k)] = \left[\alpha_k \cdot e^{j(\varphi(k) + \Delta\phi_n)}\right] k, n = 0, 1, \ldots, N-1, \tag{9}$$

where $\alpha_k \in \mathbb{R}^+$, $\varphi(k)$ and $\Delta\phi_n \in [0, 2\pi)$, $\Delta\phi_0 = \Delta\phi_{0,0} = 0$. Note that the matrix $\boldsymbol{C}^{-1}$ is a constant modulus matrix when $\alpha_k = 1$.

Such a transform matrix can always map or multiplex any original symbol vector into a constant modulus OFDM frame vector. However, this matrix is not invertible because the rank of such a matrix is 1, and the data symbol vector cannot be recovered at the receiver [19]. In order to make the matrix $\boldsymbol{C}^{-1}$ invertible, we adjust the diagonal elements of the matrix $\boldsymbol{C}^{-1}$ to be constant but non-unit amplitude $\alpha$, and the remaining elements to have another amplitude $\beta$ such that it has the full rank $N$. Moreover, if all rows or columns of such a matrix are permutated, it still maintains the full rank property [20]. The PAPR of the OFDM frame vector also remains the same. Accordingly, the modified matrix $\boldsymbol{C}^{-1}$ can be designed in different permutation forms of the initial adjusted matrix that provides many possible transformation sets as presented in part (c).

After modification on the amplitudes of the matrix $\boldsymbol{C}^{-1}$, those data symbols generated from the $M$-PSK can be transformed into a constant modulus OFDM frame when setting $\beta$ to be zero. Although the $M$-QAM modified symbols cannot be multiplexed into a constant modulus OFDM frame, a significant improvement on the PAPR compared to the PTS, SLM and WHT still can be shown as follows.

(c) Define a given permutation $\tilde{N}$ with $N$ elements that $\tilde{N}:\{0, 1, \ldots, N-1\} \to \{0, 1, \ldots, N-1\}$ [21]. For example, the permutated order may be $\tilde{N}:\{2, 0, 3, 1\}$ when $N = 4$. We employ the modified matrix $\tilde{\boldsymbol{C}}^{-1}$ that is invertible as follows

$$\tilde{c}_n(k) = \begin{cases} \alpha \cdot e^{j(\varphi(k)+\Delta\phi_n)} & k = \tilde{N}(n)\, k, n = 0, \ldots, N-1 \\ \beta \cdot e^{j(\varphi(k)+\Delta\phi_n)} & k \neq \tilde{N}(n) \end{cases} \\ = \alpha^{I_{\tilde{N}(n)}(k)} \cdot \beta^{1-I_{\tilde{N}(n)}(k)} \cdot e^{j(\varphi(k)+\Delta\phi_n)}, \tag{10}$$

where $\alpha \in (0, \infty), \beta \in [0, \infty), \alpha > \beta, \varphi(k)$ and $\Delta\phi_n \in [0, 2\pi), \Delta\phi_0 = 0$, let $\varphi(k) = \varphi(0) + A_k\pi$ for simplicity and $A_k \in \mathbb{Z}$. $I_n(k)$ is called *indicator function* [22], having the value 1 for element $k$ equals to element $n$ and the value 0 for element $k$ different than $n$, which is defined as

$$I_n(k) = \begin{cases} 1 & \text{if } k = n \\ 0 & \text{if } k \neq n \end{cases}. \tag{11}$$

To express the modified matrix $\tilde{\boldsymbol{C}}^{-1}$ more intuitively, let vector $\underline{\boldsymbol{\eta}}^{\mathrm{T}} = [e^{j\varphi(k)}]_{k=0}^{N-1}$, vector $\underline{\boldsymbol{\psi}}^{\mathrm{T}} = \left[e^{j\Delta\phi_n}\right]_{n=0}^{N-1}$, matrix $\boldsymbol{\Sigma}_1 = \mathrm{diag}\left(\underline{\eta}\right)$, $\boldsymbol{\Sigma}_2 = \mathrm{diag}\left(\underline{\boldsymbol{\psi}}\right)$ and a real matrix

$$\boldsymbol{\Gamma} = \begin{pmatrix} \alpha & & \beta \\ & \ddots & \\ \beta & & \alpha \end{pmatrix}_{N\times N}, \tag{12}$$

with its arbitrarily permutated columns as

$$\boldsymbol{\Gamma} = \begin{pmatrix} \beta & \ldots & \alpha & \ldots & \beta \\ \beta & \ldots & \ldots & \beta & \alpha \\ \vdots & \alpha & \ldots & \ldots & \vdots \\ \beta & \ldots & \ldots & \alpha & \beta \\ \alpha & \beta & \ldots & \ldots & \beta \end{pmatrix}_{N\times N}. \tag{13}$$

Then, the inverse matrix $\tilde{\boldsymbol{C}}^{-1} = \boldsymbol{\Sigma}_1\boldsymbol{\Gamma}\boldsymbol{\Sigma}_2$.

Therefore, there are two possible cases that can be pursued. Namely, case 1 where amplitude $\beta$ is positive real number, the matrix $\tilde{\boldsymbol{C}}^{-1}$ can be normalised to

$$\tilde{c}_n(k) = \tilde{\alpha}^{I_{\tilde{N}(n)}(k)} \cdot e^{j(\varphi(k)+\Delta\phi_n)}, \tag{14}$$

here $\tilde{\alpha} = \alpha/\beta$. For readability, we still use $\alpha$ instead of $\tilde{\alpha}$. In case 2 where $\beta$ is zero, the matrix $\tilde{\boldsymbol{C}}^{-1}$ becomes a constant modulus diagonal matrix

$$\tilde{c}_n(k) = \begin{cases} \alpha \cdot e^{j(\varphi(k)+\Delta\phi_n)} & k = \tilde{N}(n) \\ 0 & k \neq \tilde{N}(n) \end{cases} \\ k, n = 0, \ldots, N-1. \tag{15}$$

Due to the property imposed in the design of matrix $\tilde{\boldsymbol{C}}^{-1}$, amplitudes of all components in an OFDM frame vector are

$$\begin{aligned} |x(n)| &= \left| e^{j\Delta\phi_n} \sum_{k=0}^{N-1} \alpha^{I_{\tilde{N}(n)}(k)} \cdot \beta^{1-I_{\tilde{N}(n)}(k)} \cdot X(k) \cdot e^{j\varphi(k)} \right| \\ &= \left| \sum_{k=0}^{N-1} \alpha^{I_{\tilde{N}(n)}(k)} \cdot \beta^{1-I_{\tilde{N}(n)}(k)} \cdot X(k) \cdot e^{j\varphi(k)} \right| \\ &= \begin{cases} \left| \sum_{k=0}^{N-1} \alpha^{I_{\tilde{N}(n)}(k)} \cdot X(k) \cdot e^{j\varphi(k)} \right| & \beta = 1 \\ \alpha \left| X(\tilde{N}(n)) \right| & \beta = 0 \end{cases}. \end{aligned} \tag{16}$$

Suppose the permutation $\tilde{N}(n) = k_1$, $\tilde{N}(m) = k_2$, $k_1 \neq k_2$ for the $n$th and the $m$th components of the OFDM frame. Based on the theorem [23] $||a| - |b|| \leq |a - b|$, the amplitude difference between these two components is derived as

$$\begin{aligned} \left| |x(n)| - |x(m)| \right| &= \left| |S_1| - |S_2| \right| \leq |S_1 - S_2| \\ &= |\hat{S}_1 - \hat{S}_2| = (\alpha - \beta)\left| X(k_1)e^{j\varphi(k_1)} - X(k_2)e^{j\varphi(k_2)} \right|, \end{aligned} \tag{17}$$

where

$$\begin{aligned} S_1 &= \alpha \cdot X(k_1)e^{j\varphi(k_1)} + \sum_{k=0, k\neq k_1}^{N-1} \beta \cdot X(k)e^{j\varphi(k)} \\ S_2 &= \alpha \cdot X(k_2)e^{j\varphi(k_2)} + \sum_{k=0, k\neq k_2}^{N-1} \beta \cdot X(k)e^{j\varphi(k)}, \end{aligned} \tag{18}$$

and

$$\begin{aligned} \hat{S}_1 &= \alpha \cdot X(k_1)e^{j\varphi(k_1)} + \beta \cdot X(k_2)e^{j\varphi(k_2)} \\ \hat{S}_2 &= \alpha \cdot X(k_2)e^{j\varphi(k_2)} + \beta \cdot X(k_1)e^{j\varphi(k_1)}. \end{aligned} \tag{19}$$

The original symbol vector $\underline{\boldsymbol{X}} = [X(0), X(1), \ldots, X(N-1)]^{\mathrm{T}}$ is generated from an $M$-point SA constellation such as $M$-PSK or $M$-QAM. Here, since $\varphi(k) = \varphi(0) + A_k\pi$ such that $\{X(k)e^{j\varphi(k)}, k = 0, 1, \ldots, N-1\} \in \{M\text{-PSK or } M\text{-QAM shifted by } \varphi(0)\}$. Therefore, $|X(k_1)e^{j\varphi(k_1)} - X(k_2)e^{j\varphi(k_2)}|$ has no more than $M$ possible values in the SA modulation. Note that when $\alpha$ is large, those components amplitudes will be dominated by and approximately equivalent to the largest symbol in each summation function of (16). Accordingly, for case 1 ($\beta = 1$) the difference between arbitrary two components will be

$$\begin{aligned} ||x(n)| - |x(m)|| &\simeq \left| \left|\alpha X(k_1)e^{j\varphi(k_1)}\right| - \left|\alpha X(k_2)e^{j\varphi(k_2)}\right| \right| \\ &= \alpha \left| |X(k_1)| - |X(k_2)| \right|. \end{aligned} \tag{20}$$

As a result, this is approximately the same as case 2 ($\beta = 0$). Due to the axial symmetry in the $M$-point SA constellation, the amplitude value of the OFDM component yields no more than $M/4$ possible values for $M$-QAM and only one value for $M$-PSK with $\alpha$ times value increase on the original constellation. After the normalisation for case 2, the parameter $\alpha = 1$. From (17), it is observed that the PAPR performance is independent of the phase vector $\underline{\boldsymbol{\psi}}$ in matrix $\tilde{\boldsymbol{C}}^{-1}$, and also independent of the phase vector $\underline{\boldsymbol{\eta}}$ in (20).

Compared to the original OFDM frame which is multiplexed by the inverse DFT matrix, the amplitude values of the OFDM frame have many more possibilities. The amplitudes of the OFDM frame modified by the inverse DFT (original OFDM frame) and the proposed matrix $\tilde{\boldsymbol{C}}^{-1}$ in the time domain are shown in Fig. 1 ($\alpha = 100$ is taken for case 1 and $\alpha = 1$ in case 2). It is seen that amplitudes of OFDM frame modified by the proposed matrix $\tilde{\boldsymbol{C}}^{-1}$ are more concentrated and less fluctuating in the time domain. Accordingly, the PAPR performance is significantly improved.

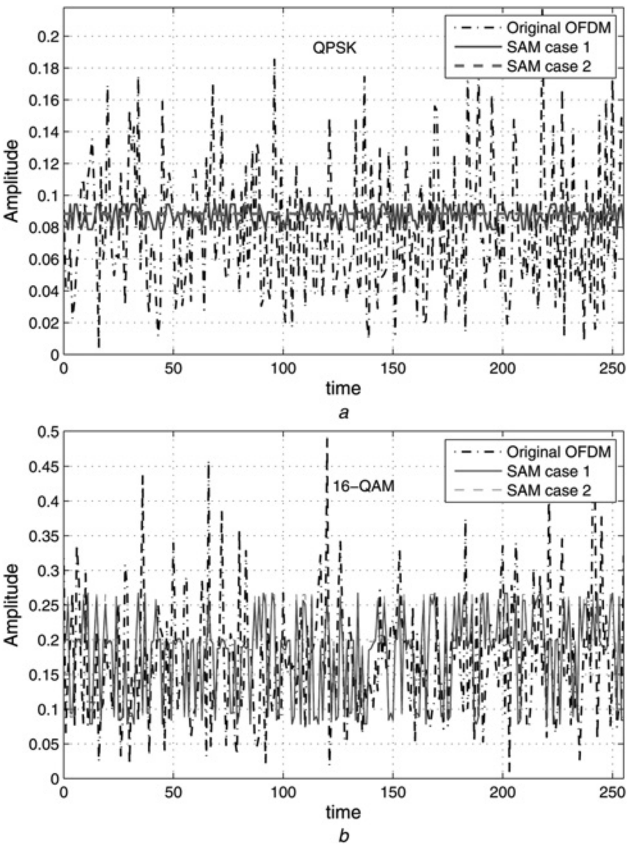


**Fig. 1** *Amplitudes of the OFDM frame for*

*a) QPSK and*
*b) 16-QAM*

Since this method allows OFDM frame vector elements to get their amplitude values from an $M$/4-valued SA, it reduces PAPR. Moreover, it provides an invertible matrix $\tilde{\boldsymbol{C}}^{-1}$ and its inverse is used at the receiver. Also note that while $\alpha$ goes to infinity, the matrix $\tilde{\boldsymbol{C}}^{-1}$ becomes identical to case 2: as a constant modulus diagonal matrix or permutated ones. Under case 2, all constant power symbols, e.g. $M$-PSK, will be transformed into constant modulus OFDM frames that meet the design objectives.

(d) Now, we factor $\tilde{\boldsymbol{C}}^{-1}$ into an inverse DFT matrix $\boldsymbol{A}_{\text{DFT}}^{-1}$ and a matrix $\boldsymbol{B}^{-1}$ since the OFDM system needs to be built up with utilisation of the IFFT operator. The invertible matrix $\boldsymbol{B}^{-1}$ is called symbol alphabet modifier matrix and is expressed as

$$\begin{aligned} \tilde{\boldsymbol{C}}^{-1} &= \boldsymbol{A}_{\text{DFT}}^{-1} \cdot \boldsymbol{B}^{-1} \quad \tilde{\boldsymbol{C}} \cdot \tilde{\boldsymbol{C}}^{-1} = I \\ \boldsymbol{B}^{-1} &= \boldsymbol{A}_{\text{DFT}} \cdot \tilde{\boldsymbol{C}}^{-1} \quad \boldsymbol{B} \cdot \boldsymbol{B}^{-1} = I \end{aligned}, \tag{21}$$

where $\boldsymbol{B}^{-1}$ is derived as

$$\begin{aligned} \boldsymbol{B}^{-1} &= \left[\tilde{b}_k(n)\right]_{\text{SAM}}, \quad k, n = 0, 1, \ldots, N-1 \\ \tilde{b}_k(n) &= \sum_{l=0}^{N-1} \mathrm{e}^{-\mathrm{j}2\pi kl/N} \cdot \tilde{c}_n(l) \\ &= \sum_{l=0}^{N-1} \alpha^{I_{\tilde{N}(n)}(l)} \cdot \beta^{1-I_{\tilde{N}(n)}(l)} \cdot \mathrm{e}^{\mathrm{j}\left(\varphi(l)+\Delta\phi_n-2\pi kl/N\right)}, \\ \beta &= \{0, 1\}. \end{aligned} \tag{22}$$

In case 2, the SAM matrix $\boldsymbol{B}^{-1}$ is an orthogonal matrix. In case 1, the SAM matrix $\boldsymbol{B}^{-1}$ is not a constant modulus matrix which modifies the amplitude as well as average power of the original symbols. One can normalise the power of the modified symbols close to the original ones before the IFFT operator by dividing with a factor of Frobenius norm $\left\|\boldsymbol{B}^{-1}\right\|_{\text{F}}/\sqrt{N}$ [24]. We rewrite the SAM matrix $\boldsymbol{B}^{-1}$ as

$$\begin{aligned} \boldsymbol{B}^{-1} &= \left[\frac{\tilde{b}_k(n)}{\sqrt{\sum_{k=0}^{N-1}\sum_{n=0}^{N-1}\left|\tilde{b}_k(n)\right|^2/N}}\right]_{\text{SAM}} \\ k, n &= 0, 1, \ldots, N-1. \end{aligned} \tag{23}$$

The estimation of received data symbols can be obtained as

$$\boldsymbol{Y} = \boldsymbol{B} \cdot \boldsymbol{B}^{-1}\boldsymbol{X} + \boldsymbol{B} \cdot \boldsymbol{W}_0 = \boldsymbol{I} \cdot \boldsymbol{X} + \boldsymbol{B} \cdot \boldsymbol{W}_0, \tag{24}$$

where $\boldsymbol{W}_0$ denotes complex additive white Gaussian noise (AWGN) vector with zero mean and variance $\sigma_{w_0}^2$.

At the receiver, after passing through the inverse SAM matrix (orthogonal), $E[(\boldsymbol{W}_0^{\text{H}}\boldsymbol{B}^{\text{H}})(\boldsymbol{B}\boldsymbol{W}_0)] = E[\boldsymbol{W}_0^{\text{H}}\boldsymbol{W}_0] = \sigma_{w_0}^2\boldsymbol{I}$, where $[\cdot]^{\text{H}}$ denotes the Hermitian conjugate operator, $\boldsymbol{I}$ is the identity matrix, the noise vector $\boldsymbol{B}\boldsymbol{W}_0$ has the same mean and variance as AWGN vector $\boldsymbol{W}_0$. Accordingly, the proposed SAM matrix will not cause BER degradation in AWGN channel which can be shown in the

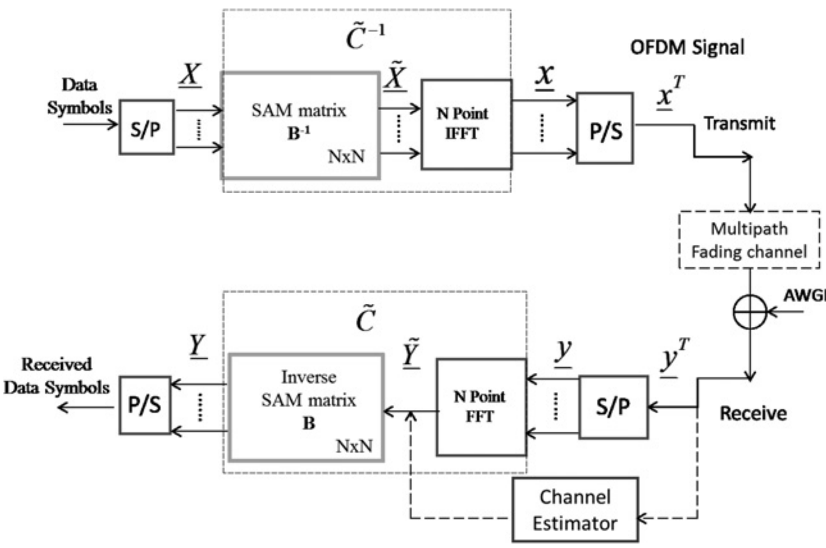


**Fig. 2** *Block diagram of the OFDM system with the proposed PAPR reduction method*

**Table 1** Average power variations of SAM in two cases, PTS, SLM, A-SLM and WHT for QPSK and 16-QAM with $N = 64$

| $N = 64$ | Power varied (QPSK), dB | Power varied (16-QAM), dB |
|---|---|---|
| WHT | 0 | 0 |
| PTS | 0 | 0 |
| SLM | 0 | 0 |
| A-SLM | 2.5 | 4.2 |
| SAM[1] $\alpha > 10^3$ | $<10^{-3}$ | $<10^{-3}$ |
| SAM[1] $\alpha = 100$ | 0.03 | 0.1 |
| SAM[2] | 0 | 0 |

following section. Fig. 2 displays the block diagram of the proposed OFDM system.

*Remark:* It is observed that when $\boldsymbol{B}^{-1}$ is a constant modulus diagonal matrix, it represents one of the phase sequences in the ordinary SLM technique. Moreover, the matrix factorisation in (21) leads to the generalised DFT (GDFT) framework reported in [25] as follows

$$\boldsymbol{A}_{\mathrm{GDFT}}^{-1} = \boldsymbol{A}_{\mathrm{DFT}}^{-1} \cdot G^{-1} = \left[\mathrm{e}^{\mathrm{j}2\pi kn/N} \cdot g_{k,n}\mathrm{e}^{\mathrm{j}\theta_{k,n}}\right] \quad k, n = 0, 1, \ldots, N-1. \tag{25}$$

## 4 PAPR and BER performance comparisons

The performance simulation results are presented in this section. Table 1 tabulates the average power fluctuation (in dB) of the proposed SAM in two cases (superscripts 1 and 2 denote for case 1 and case 2, respectively), WHT, PTS, SLM, A-SLM methods for QPSK and 16-QAM with $N = 64$ subcarriers. In the A-SLM, the number of amplitude modified symbols in each sequence is uniformly distributed in the interval $[0, S_{\max}]$ where parameters $S_{\max} = 6$, $D = 2.4$ with QPSK and $D = 4.4$ with 16-QAM, were used as suggested in [9]. As seen from the table: in case 1, when the value of $\alpha$ is larger, the power fluctuation of OFDM frame is approaching zero. In case 2, the SAM matrix $\boldsymbol{B}^{-1}$ is orthogonal, so the power of the original symbols will not be changed with power normalisation. The OFDM system simulations were performed for both cases (choose $\alpha = 100$ in case 1, $\alpha = 1$ in case 2) of the proposed SAM method with $\varphi(0) \in [0, 2\pi)$ as selected randomly, and choosing $\varphi(l) = \varphi(0) + l\pi$, $\Delta\phi_n = n\pi/4$ in function (22), where the permutation $\tilde{N}$ is arbitrarily generated.

The complexities of various methods considered in this paper are tabulated in Table 2. In PTS and SLM techniques, $U$ and $V$ IFFT operations are required. Also, SI bits are used. On the other hand, the proposed SAM needs only one IFFT operation and no SI bits are required at the receiver. The DFT of the modified matrix $\tilde{\boldsymbol{C}}^{-1}$ yields the SAM matrix as shown in (21). In the calculation of $\tilde{\boldsymbol{C}}^{-1}$, $\boldsymbol{\eta}^{\mathrm{T}} = \left[\mathrm{e}^{\mathrm{j}\varphi(l)}\right]_{l=0}^{N-1}$ and $\boldsymbol{\psi}^{\mathrm{T}} = \left[\mathrm{e}^{\mathrm{j}\Delta\phi_n}\right]_{n=0}^{N-1}$ totally requires $2N$ multiplications and zero additions. When $\varphi(l) = \Delta\phi_n = 0$, zero multiplications and additions are needed. Matrix $\boldsymbol{\Gamma}$ requires $N$ multiplications and $2N$–1 additions for case 1 (where $\beta = 1$), and no multiplications and additions for case 2 (where $\alpha = 1$, $\beta = 0$). In addition, FFT operation requires $N/2\log_2(N)$ multiplications and $N\log_2(N)$ additions. Apparently, the proposed method has much lower computational complexity than the other methods as also plotted in Fig. 3.

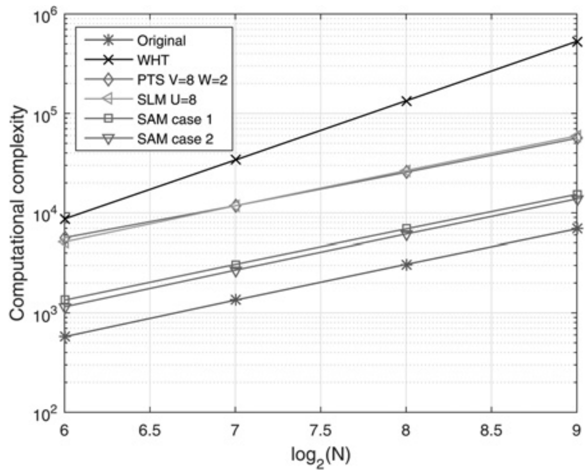


**Fig. 3** *Computational complexity of the proposed SAM (two cases), WHT-OFDM, PTS and ordinary SLM methods*

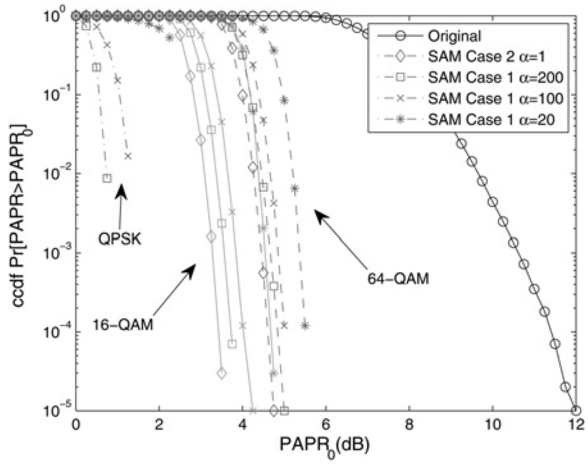


**Fig. 4** *PAPR performance of the proposed SAM in two cases for QPSK, 16-QAM, 64-QAM and N = 128 in the OFDM system*

Fig. 4 displays the PAPR performance of the proposed method along with different parameter values for two cases. Figs. 5 and 6 illustrate the CCDFs performance of the proposed SAM, WHT-OFDM, PTS, ordinary SLM and A-SLM methods. For QPSK and subcarriers $N = 128$, the OFDM candidates in the SLM and A-SLM have $U = 8$ and 64, $S_{\max} = 12$, $D = 2.4$, while

**Table 2** System complexity of SAM, PTS, SLM and WHT methods for the OFDM system

| $N = 64$ | Number of complex multiplications | Number of complex additions | SI, bit | Number of IFFTs |
|---|---|---|---|---|
| original | $\frac{N}{2}\log_2(N)$ | $N\log_2(N)$ | no | 1 |
| WHT | $\frac{N}{2}\log_2(N) + N^2$ | $N\log_2(N) + N(N-1)$ | no | 1 |
| PTS | $\frac{VN}{2}\log_2(N) + VW^{V-1}$ | $VN\log_2(N)$ | yes | $V$ |
| SLM | $\frac{UN}{2}\log_2(N) + UN$ | $UN\log_2(N)$ | yes | $U$ |
| SAM[1] | $N\log_2(N) + N$ | $2N\log_2(N) + 2N - 1$ | no | 1 |
| SAM[2] | $N\log_2(N)$ | $2N\log_2(N)$ | no | 1 |

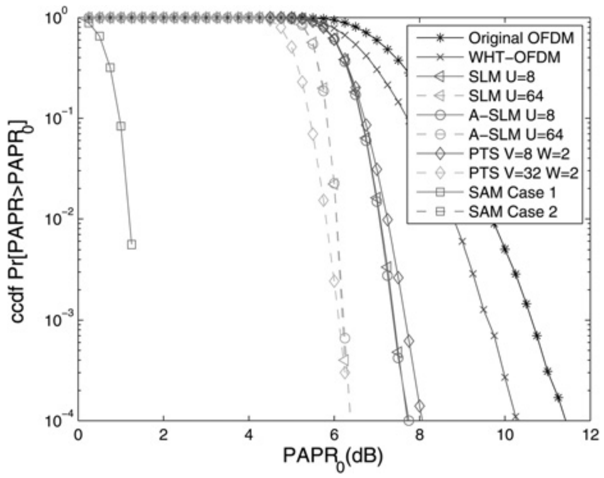


**Fig. 5** *PAPR performance of the proposed SAM in two cases, WHT-OFDM, PTS, ordinary SLM and A-SLM methods for QPSK and N = 128*

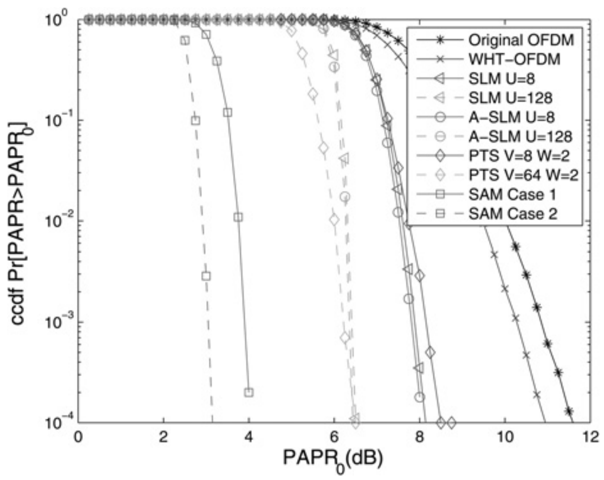


**Fig. 6** *PAPR performance of the proposed SAM in two cases, WHT-OFDM, PTS, ordinary SLM and A-SLM methods for 16-QAM and N = 256*

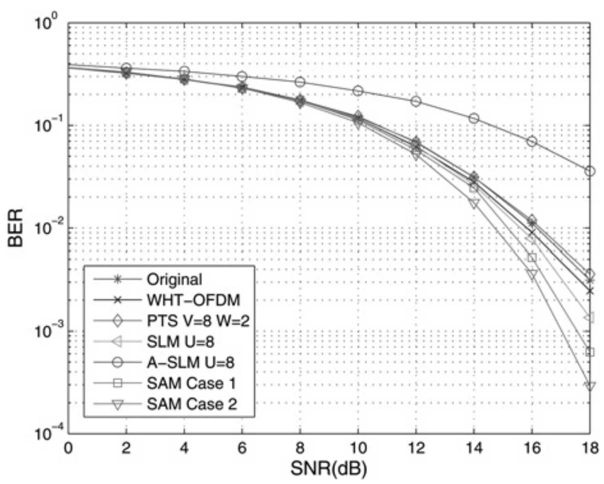


**Fig. 7** *BER performance comparisons of the proposed SAM in two cases, WHT-OFDM, PTS, ordinary SLM and A-SLM methods for 16-QAM and N = 256 over AWGN channel*

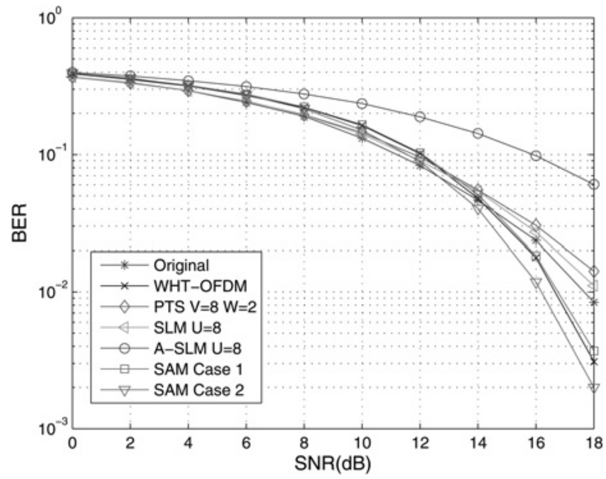


**Fig. 8** *BER performance comparisons of the proposed SAM in two cases, WHT-OFDM, PTS, ordinary SLM and A-SLM methods for 16-QAM and N = 256 over multi-path fading channel*

subblocks $V = 8$ and 32, phase coefficients $W = 2$ are used for PTS. Also $U = 8$ and 128, $S_{max} = 25$, $D = 4.4$, $V = 8$ and 64, $W = 2$ for 16-QAM and $N = 256$, respectively. The CCDFs are simulated by randomly generating 100,000 OFDM frames for each method.

Figs. 7 and 8 display the BER performance comparisons over the AWGN channel and the multipath fading channel with high PA (HPA). The multipath fading channel is assumed to be a three-path Rayleigh fading channel with equal power. The HPA is modelled as Rapp's solid state PA (SSPA) given as [26], the output signal of the SSPA is defined as

$$r_{out} = \frac{r_{in}}{\left(1 + r_{in}^{2p}\right)^{1/2p}}, \tag{26}$$

where $r_{in}$ and $r_{out}$ denote the amplitude of input and output signals, respectively, choose $p = 2$ to approximate a practical HPA [26].

These performance results confirm that the proposed SAM method significantly outperforms PTS, SLM and WHT techniques in PAPR reduction. Case 2 as the ultimate form of case 1, at the CCDF rate of $10^{-3}$ as a threshold, yields a PAPR of 0 dB for QPSK and 3 dB for 16-QAM. Case 1 yields 0.8 dB for QPSK and 3.9 dB for 16-QAM, whereas the original OFDM signal is 10.2 and 11.1 dB, respectively. An outstanding PAPR improvement is achieved by the proposed SAM method especially in case 2 that offers the best performance in PAPR reduction without BER degradation. Hence, the OFDM system with the proposed SAM method reduces power consumption of HPA and avoids BER degradation caused by in-band interference. Note that the PTS and SLM methods require SI bits to be transmitted without any error tolerance such that the receiver can recover the original data without failure. On the other hand, the SAM method does not need to reserve bits for the transmission of the SI, resulting in the increase of the data rate, and simple to implement.

## 5 Conclusions

In this paper, a new PAPR reduction method is proposed based on the phase and amplitude modifications in the SA, only utilising a predesigned SAM matrix along with a single IFFT/FFT pair in the OFDM system. The SAM technique provides a dramatic reduction in PAPR performance and outperforms the WHT, PTS and SLM-based methods, especially for case 2 implementation that forms an orthogonal SAM matrix. Moreover, the proposed method has low-complexity to implement and does not require any SI.

## 6 References


1 Akansu, A.N., Duhamel, P., Lin, X.M., *et al.*: 'Orthogonal transmultiplexers in communication: a review', *IEEE Trans. Signal Process., Spec. Issue Theory Appl. Filter Banks Wavelets*, 1998, **46**, (4), pp. 979–995

2 Haddad, R.A., Akansu, A.N.: 'Multiresolution signal decomposition: transforms, subbands, and wavelets' (Academic Press, 1992)

3 Lim, D., Heo, S., No, J.: 'An overview of peak-to-average power ratio reduction schemes for OFDM signals', *J. Commun. Netw.*, 2009, **11**, (3), pp. 229–239

4 Muller, S.H., Huber, J.B.: 'OFDM with reduced peak-to-average power ratio by optimum combination of partial transmit sequences', *Electron. Lett.*, 1997, **33**, (5), pp. 368–369

5 Cimini, L.J., Sollenberger, N.R.: 'Peak-to-average power ratio reduction of an OFDM signal using partial transmit sequences', *IEEE Commun. lett.*, 2000, **4**, (3), pp. 86–88

6 Le Goff, S.Y., Boon, K.K., Tsimenidis, C.C., *et al.*: 'A novel selected mapping technique for PAPR reduction in OFDM systems', *IEEE Trans. Commun.*, 2008, **56**, (11), pp. 1775–1779

7 Bauml, R.W., Fischer, R.F.H., Huber, J.B.: 'Reducing the peak-to-average power ratio of multicarrier modulation by selected mapping', *Electron. Lett.*, 1996, **32**, (22), pp. 2056–2057

8 Yew, K.M., Drieberg, M., Jeoti, V.: 'On PAPR reduction in OFDM systems: A technique using normalized complex Hadamard transform'. TENCON 2005 IEEE Region 10, Melbourne, Australia, November 2005, pp. 21–24

9 Cho, Y.C., Han, S.H., Lee, J.H.: 'Selected mapping technique with novel phase sequences for PAPR reduction of an OFDM signal'. IEEE 60th Vehicle Technology Conf. (VTC2004-Fall), Los Angeles, USA, September 2004, 7, pp. 4781–4785

10 Sharif, M., Florens, C., Fazel, M., *et al.*: 'Amplitude and sign adjustment for peak-to-average-power reduction', *IEEE Trans. Commun.*, 2005, **53**, (8), pp. 1243–1247

11 Yang, L., Alsusa, E.: 'Novel low-complexity post-IFFT PAPR reduction technique by utilizing amplitude transforming for OFDM systems'. IEEE Wireless Communications and Networking Conf. (WCNC), Kowloon, Hongkong, March 2007, pp. 1339–1343

12 Yang, L., Liu, J., Zhang, L.: 'Low-complexity time domain PAPR mitigation by amplitude modification for OFDM systems'. IEEE 72th Vehicle Technology Conf. (VTC2000-Fall), Ottawa, Canada, September 2010, pp. 1–5

13 Jiang, T., Xiang, W., Richardson, *et al.*: 'PAPR reduction of OFDM signals using partial transmit sequences with low computational complexity', *IEEE Trans. Broadcast.*, 2007, **53**, (3), pp. 719–724

14 Yang, L., Soo, K.K., Li, S.Q., *et al.*: 'PAPR reduction using low complexity PTS to construct of OFDM signals without side information', *IEEE Trans. Broadcast.*, 2011, **57**, (2), pp. 284–290

15 Kojima, T., Iwamoto, S., Shida, Y., *et al.*: 'A novel SLM PAPR reduction of OFDM signals without side information'. IEEE Int. Symp. on Signal Processing and Information Technology (ISSPIT), Luxor, Egypt, December 2010, pp. 321–325

16 Su, S., Lee, C., Lin, C., *et al.*: 'A novel PAPR reduction scheme without side information by using linear phase rotation vector'. IEEE Wireless Communications and Networking Conf. (WCNC), Shanghai, China, April 2013, pp. 4048–4052

17 Breiling, H., Muller-Weinfurtner, S.H., Huber, J.B.: 'SLM peak power reduction without explicit side information', *IEEE Commun. Lett.*, 2001, **5**, (6), pp. 239–241

18 Kaur, P., Singh, R.: 'Complementary cumulative distribution function for performance analysis of OFDM signal', *IOSR J. Electon. Commun. Eng. (IOSRJECE)*, 2012, **2**, (5), pp. 5–7

19 Atkinson Kendall, A.: 'An introduction to numerical analysis' (John Wiley & Sons Press, New York, 1989, 2nd edn.)

20 Brualdi, R.A.: 'Combinatorial matrix classes' (Cambridge University Press, 2006), p. 19

21 Miklos, B.: 'Combinatorics of permutations' (Chapman and Hall-CRC Press, 2004, 2012, 2nd edn.)

22 Folland, G.B.: 'Real analysis: modern techniques and their applications' (John Wiley & Sons Press, 1999, 2nd edn.)

23 Rudin, W.: 'Principles of mathematical analysis' (New York: McGraw-Hill Press, 1976)

24 Demmel, J.W.: 'Applied numerical linear algebra' (SIAM Press, 1997), section 1.7

25 Akansu, A.N., Agirman-Tosun, H.: 'Generalized discrete Fourier transform with nonlinear phase', *IEEE Trans. Signal Process.*, 2010, **58**, (9), pp. 4547–4556

26 Costa, E., Midrio, M., Pupolin, S.: 'Impact of amplifier nonlinearities on OFDM transmission system performance', *IEEE Commun. Lett.*, 1999, **3**, (2), pp. 37–39